Editors' Suggestion

Emergence of Competing Orders and Possible Quantum Spin Liquid in SU(N) Fermions

Xue-Jia Yu,[1,2] Shao-Hang Shi,[3,4] Limei Xu,[1,5,6] and Zi-Xiang Li[3,4,*]

[1]International Center for Quantum Materials, School of Physics, Peking University, Beijing 100871, China
[2]Fujian Key Laboratory of Quantum Information and Quantum Optics, College of Physics and Information Engineering, Fuzhou University, Fuzhou, Fujian 350108, China
[3]Beijing National Laboratory for Condensed Matter Physics and Institute of Physics, Chinese Academy of Sciences, Beijing 100190, China
[4]University of Chinese Academy of Sciences, Beijing 100049, China
[5]Collaborative Innovation Center of Quantum Matter, Beijing 100871, China
[6]Interdisciplinary Institute of Light-Element Quantum Materials and Research Center for Light-Element Advanced Materials, Peking University, Beijing 100871, China

(Received 29 November 2022; revised 26 November 2023; accepted 1 December 2023; published 18 January 2024)

In the past few decades, tremendous efforts have been made toward understanding the exotic physics emerging from competition between various ordering tendencies in strongly correlated systems. Employing state-of-the-art quantum Monte Carlo simulation, we investigate an interacting SU(N) fermionic model with varying interaction strength and value of N, and we unveil the ground-state phase diagram of the model exhibiting a plethora of exotic phases. For small values of N—namely, $N = 2, 3$—the ground state is an antiferromagnetic (AFM) phase, whereas in the large-N limit, a staggered valence bond solid (VBS) order is dominant. For intermediate values of N such as $N = 4, 5$, remarkably, our study reveals that distinct VBS orders appear in the weak and strong coupling regimes. More fantastically, the competition between staggered and columnar VBS ordering tendencies gives rise to a Mott insulating phase without spontaneous symmetry breaking (SSB), existing in a large interacting parameter regime, which is consistent with a gapped quantum spin liquid. Our study not only provides a platform to investigate the fundamental physics of quantum many-body systems—it also offers a novel route toward searching for exotic states of matter such as quantum spin liquid in realistic quantum materials.

DOI: 10.1103/PhysRevLett.132.036704

Introduction.—Understanding competing orders arising from strong electronic interactions plays a vital role in fathoming the fundamental theory of quantum many-body physics [1,2], as well as many appealing phenomena in quantum materials, including high-T_c superconductivity [3–5]. More intriguingly, the competitions between various ordering tendencies offer a route toward yielding exotic states of matter. A typical example is quantum spin liquid (QSL) [6–11], a Mott insulating phase featuring deconfined fractionalization, without symmetry spontaneously breaking even at zero temperature. Despite vigorous studies in past decades [12–34], most of them focus on spin systems, and in particular, QSL has been revealed to be realized in realistic spin models [32]. An unambiguous demonstration of realizing QSL in realistic fermionic models by an unbiased theoretical approach remains elusive.

On a different front, another promising mechanism to trigger exotic states of matter is assigning more degrees of freedom to the microscopic models and extending symmetries. By extending the spin symmetry group SU(2) in an electronic spin system to SU(N), it is theoretically predicted that the quantum fluctuation of the spin is enhanced with increasing N [35,36], rendering the possibility of exotic quantum paramagnetic phases such as valence bond solids [37–41] and QSLs [27,42,43]. Fruitful, fascinating physics is revealed in the interacting SU(N) systems by virtue of the cooperative effects of enlarged symmetry and strong correlation [44–74]. Benefiting from celebrated progresses in cold-atom experiments, various SU(N) symmetric systems are realized in an optical lattice [75–81]. More recently, enlarged SU(N) symmetry is proposed to emerge in the twisted bilayer graphene system [82–84] as a low-energy effective description combining spin and valley degrees of freedom [85–88]. Hence, designing a concrete model with extended symmetry and investigating the effect of strong correlation in a theoretically controlled approach is vastly desired.

In this Letter, we construct a SU(N) interacting fermionic model on a square lattice. Remarkably, the model is sign-problem free at half filling for any N [89–92], and is thus amendable to approximation-free quantum Monte Carlo (QMC) simulation [93–95] at low temperature (or zero temperature) with large system sizes. We perform a large-scale projector QMC simulation and investigate ground-state properties of the model with varying interaction strengths and values of N. At small values of N, the

ground state is an antiferromagnetic (AFM) spin ordered state, like the SU(2) Heisenberg model on a square lattice. With increasing N, the quantum fluctuation of spin destroys spin long-range order, creating valence bond solid (VBS) ordering that breaks translational symmetry while preserving spin rotational symmetry. The most intriguing phenomena occur with intermediate values of N, wherein the insulating phases in the weakly coupling regime and strongly coupling regime feature distinct patterns of VBSs. The competition between the two ordering tendencies gives rise to an intermediate insulating phase without any spontaneous symmetry breaking (SSB) even at zero temperature. Such a symmetric Mott insulator is a possible gapped QSL phase featuring topological order [96–99].

Model and method.—We consider the following interacting microscopic model of SU(N) fermions on the square lattice [known as the Su-Schrieffer-Heeger (SSH) interacting model] [100]:

$$H = -t\sum_{\langle ij\rangle,\alpha}(c^{\dagger}_{i\alpha}c_{j\alpha} + \text{H.c.}) - \frac{J}{2N}\sum_{\langle ij\rangle}\left(\sum_{\alpha} c^{\dagger}_{i\alpha}c_{j\alpha} + \text{H.c.}\right)^2, \tag{1}$$

where $\langle ij\rangle$ refers to the bond between nearest-neighbor (NN) sites i and j, and $c^{\dagger}_{i\alpha}$ creates a fermion on-site i with fermion flavor labels $\alpha = 1, \ldots N$. Here, t is the fermion hopping amplitude and is set $t = 1$ as an energy unit. J represents the strength of the SSH interaction, which can be induced by SSH electron-phonon couplings in the fast-phonon limit [101,102]. Remarkably, the model in Eq. (1) is free from the notorious sign problem for any N at half filling and for even N at generic filling, and is thus a promising platform to investigate the exotic physics emerging in the SU(N) fermions. In this work, we perform unbiased, large-scale projector QMC simulation to study the ground-state properties of the model. The details of the projector QMC simulation are introduced in the Supplemental Material [103]. We focus on the model at half filling with a perfectly nested Fermi surface, and we explore the insulating phase with competing ordering arising from the interplay between the strong correlation and extended symmetry of multicomponent fermions.

Notice that for $N = 1$, the interaction in Eq. (1) is reduced to the nearest-neighbor density interaction, which favors charge-density-wave order on a bipartite lattice [104–107]. For $N = 2$, the model is a SSH electron-phonon coupling model at the antiadiabatic limit, the ground state of which is revealed to be an AFM ordered state in recent works [108–111]. In the present work, we focus on understanding the nature of the multicomponent fermions with enlarged symmetry—namely, $N \geq 3$—in the presence of strong correlation.

Quantum phase diagram.—Before presenting the details of QMC results, we summarize our main findings and the ground-state phase diagram of the model in Eq. (1).

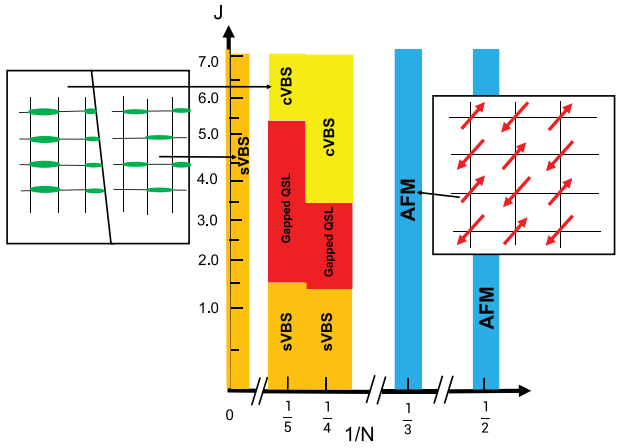

FIG. 1. Schematic ground-state phase diagram of SU(N) fermions with SSH interaction on a square lattice at half filling: for $N = 2$, 3, the ground state is an AFM ordered phase. In the large-N limit, the dominant ordering is VBS with momentum (π, π). For intermediate N values, such as $N = 4$, 5, the insulating phases in weakly and strongly interacting regimes possess VBS orders with distinct patterns of SSB. The VBS order carrying momentum (π, π) is dominant in the weakly interacting regime owing to the presence of Fermi surface nesting, while in the strongly coupling regime, a VBS order with momentum $(\pi, 0)/(0, \pi)$ appears. Most appealingly, in a large parameter regime between two VBS phases, the ground state is a Mott insulator without SSB, consistent with gapped QSL.

The schematic phase diagram with varying fermion-flavor number N is shown in Fig. 1. For small N—more explicitly, $N = 2$, 3—the ground state is an insulating phase with AFM spin long-range order. With increasing fermion-flavor number N, the quantum fluctuation of spin is enhanced, resulting in the emergence of valence bond ordering. The emergence of VBS order for the large-N case is revealed by our systematic numerical calculation. In the large-N limit, where the saddle-point approximation can render accurate results, we perform a mean-field calculation and unambiguously show that the ground state is a VBS ordered phase with momentum (π, π)—namely, a staggered VBS (sVBS) phase. In the case of large but finite N, we perform QMC simulation to decipher the rich ground-state phase diagram. For example, for $N = 4$, 5, the AFM spin order is suppressed, and VBS order becomes dominant. More strikingly, QMC simulation shows that the patterns of VBS orders in the weak and strong coupling regimes are completely different. In the weakly interacting regime, the VBS order in the ground state carries momentum (π, π) as a consequence of Fermi surface nesting. In the strongly coupling regime, the dominant pattern of VBS ordering is the columnar VBS (cVBS) with momentum $(\pi, 0)/(0, \pi)$. Appealingly, in a large interacting regime $[1.4(1.5) < J < 3.5(5.4)$ for $N = 4(5)]$, a phase without SSB arises from the competition between two VBS ordering tendencies. This phase without any SSB in the intermediate strength of J possesses finite single-particle and spin gaps. Therefore,

it is a Mott insulating phase, and possibly a QSL with exotic topological order.

Staggered VBS order in the large-N limit.—In the large-N limit for Eq. (1), the mean-field saddle-point approximation is capable of capturing the exact ground-state properties. Hence, before presenting QMC results on the finite-N system, we perform self-consistent mean-field calculation to understand the ground-state properties of Eq. (1) in the large-N limit. We decouple the interaction in Eq. (1) in the bond channel $\varphi_{x/y,i} = \langle (c_i^\dagger c_{i+\hat{x}/\hat{y}} + \text{H.c.}) \rangle$ and solve the mean-field equation self-consistently. Our calculation indicates that VBS with momentum (π, π) and VBS with momentum $(\pi, 0)/(0, \pi)$ are two dominant ordered states with close energies. We perform systematic self-consistent mean-field calculation to compare the energies of the two states, unequivocally revealing that the sVBS ordered state is energetically favored in the whole interaction parameter regime under consideration. The details and results of mean-field calculation are included in Sec. X of the Supplemental Material [103]. Furthermore, we perform QMC simulation for an extremely large N—namely, $N = 10$—and we verify that the ground state possesses sVBS order in a relatively large interacting regime (see Sec. IX of the Supplemental Material [103]), which is consistent with the saddle-point approximation calculation at the large-N limit.

AFM order for small N.—At small or intermediate values of N, quantum fluctuation beyond saddle-point approximation becomes pronounced. Consequently, an approximation-free approach incorporating the effect of quantum fluctuation is strongly desired in order to investigate the possible SSB at small or intermediate values of N. We employ numerically exact QMC simulation to explore the accurate ground-state properties of Eq. (1). To demystify various possible symmetry-breaking orders, we compute the static structure factor $S(\vec{q}, L) = (1/L^4) \sum_{i,j} e^{i\vec{q}\cdot(\vec{r}_i - \vec{r}_j)} \langle \hat{O}_i \hat{O}_j \rangle$ of the corresponding order $\hat{O}$, and L refers to the linear system size of the square lattice. The order parameter characterizing SSB is given by the peaked-momentum structure factor at the thermodynamic limit: $\Delta^2 = \lim_{L\to\infty} S(\vec{Q}_{\text{peak}}, L)$. In our study, we focus on VBS and spin orderings, the definition of which are given in Sec. I of the Supplemental Material [103]. First, the momentum distribution of the spin structure factor in Fig. 2(a) clearly displays a sharp peak at momentum (π, π), implying the existence of AFM ordering at $N = 3$. The scaling analysis of the AFM structure factor with $1/L$ unambiguously reveals the existence of AFM long-range order, as shown in Fig. 2(b), while the VBS structure factor vanishes at the thermodynamic limit. To further confirm the AFM long-range ordered ground state at $N = 3$, we perform a more sophisticated finite-size scaling procedure by calculating the RG-invariant correlation-length ratio, $R(L)_{\text{AFM/VBS}} = [S_{\text{AFM/VBS}}(\vec{Q}, L)/S_{\text{AFM/VBS}}(\vec{Q} - \delta\vec{q}, L)] - 1$, where $\vec{Q}$ labels the momentum at which the structure factor is maximum, and $\delta\vec{q} = [(2\pi/L), (2\pi/L)]$ is a minimal momentum shift from $\vec{Q}$.

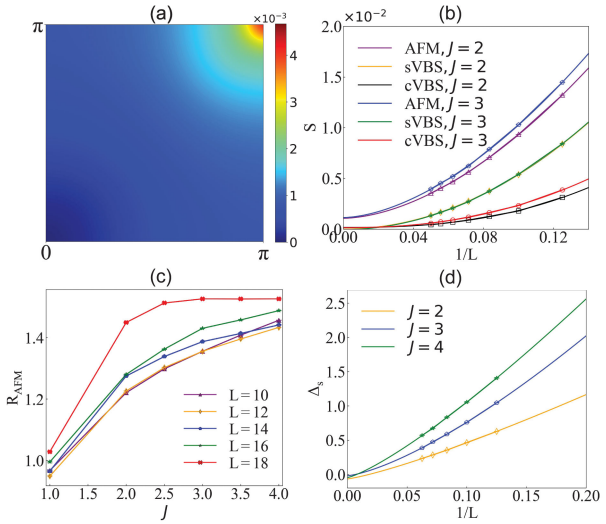

FIG. 2. Numerical evidence of AFM order for $N = 3$. (a) The momentum distribution of AFM structure factors for $J = 2$, $L = 16$, clearly showing the peak occurring at momentum (π, π). (b) Finite-size scaling of AFM, sVBS, and cVBS structure factors. The second-order polynomial is used to fit structure factors versus $1/L$, with the intercept of the extrapolation indicating the results at thermodynamic limit. (c) AFM correlation-length ratio versus interacting strength J for various system sizes. The increase of the correlation-length ratio with L is a strong evidence of long-range order. (d) The extrapolation of spin gap versus $1/L$ for $J = 2$, 3, 4. The vanishing spin gaps are consistent with AFM long-range order.

As shown in Fig. 2(c), R_{AFM} increases with system size, corroborating the existence of AFM long-range order. Conversely, the system-size dependence of the VBS correlation-length ratio, as shown in Sec. III of the Supplemental Material [103], strongly indicates the short-range property of VBS ordering at $N = 3$.

In addition to static structure factor, we investigate the spectral properties of Eq. (1) by virtue of the imaginary-time Green's function. At $N = 3$, we extract a spectral gap from the imaginary-time Green's function, with the details illustrated in Sec. II of the Supplemental Material [103]. The results of single-particle gaps at $N = 3$ with varying J are shown in the Sec. III of the Supplemental Material [103], explicitly demonstrating the existence of a finite single-particle gap at the thermodynamic limit. Furthermore, in the AFM ordered phase, the spin gap is expected to vanish at momentum (π, π) as a consequence of Goldstone modes. Figure 2(d) depicts the scaling analysis of the spin gap versus $1/L$, explicitly indicating the absence of a spin gap and corroborating the existence of AFM long-range order at $N = 3$. Our numerical results unambiguously demonstrate that the AFM order driven by SSH interaction persists up to $N = 3$ [108].

Intermediate Mott insulator without SSB.—In this section, we perform projector QMC to investigate ground-state properties of the model in Eq. (1) in the intermediate values

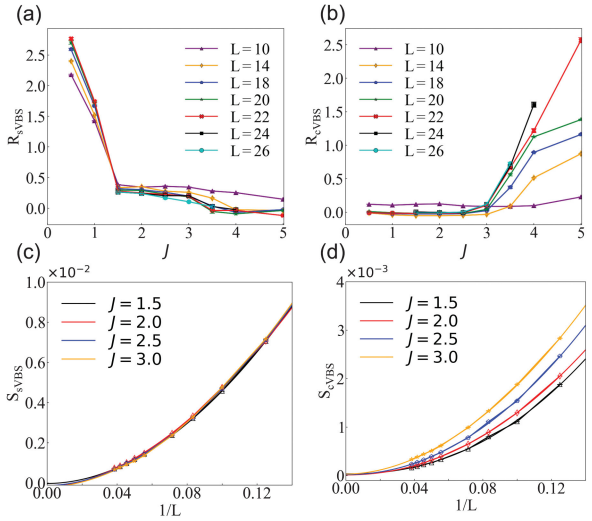

FIG. 3. The upper two graphs display the results of VBS ordering for $N = 4$: correlation length ratios of (a) sVBS and (b) cVBS. The results of sVBS increase with system size in the weakly interacting regime $J < 1.4$, indicating sVBS long-range order. The results of cVBS increase with system size in the strongly interacting regime $J > 3.5$, indicating cVBS long-range order. The lower two graphs show the finite-size scaling of (c) sVBS and (d) cVBS structure factors in the regime of intermediate interaction strength $1.4 < J < 3.5$. Both sVBS and cVBS orders vanish in the thermodynamic limit.

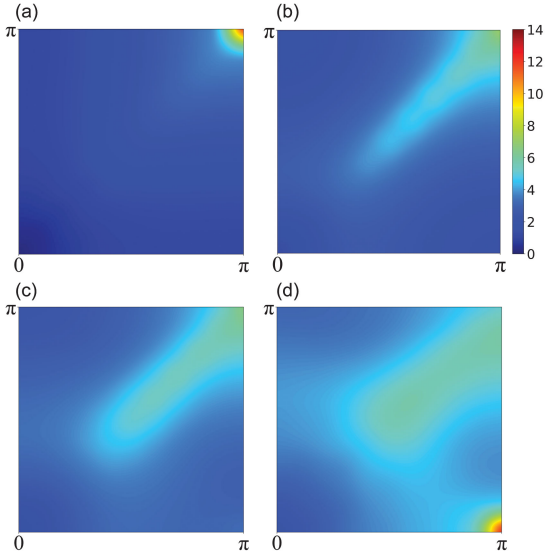

FIG. 4. Momentum distribution of VBS structure factors for $N = 4$: (a) $J = 0.5$. (b) $J = 2.0$. (c) $J = 3.0$. (d) $J = 5.0$. The linear system size is fixed as $L = 20$.

of N, wherein the competition between various ordering tendencies is expected to yield exotic phases. We first focus on $N = 4$. The results of the structure factor and correlation-length ratio clearly show that AFM order is destroyed by the quantum fluctuation of spin, included in Sec. IV of the Supplemental Material [103]. The dominant instability for $N = 4$ is VBS ordering. We present the results of the correlation-length ratio for the sVBS and cVBS orders in Figs. 3(a) and 3(b), respectively. In the weak coupling regime, the dominant VBS ordering is VBS with momentum (π, π), owing to the Fermi surface nesting on the square lattice at half filling. Remarkably, in the presence of strong interaction, the ground state displays VBS order with momentum $(\pi, 0)/(0, \pi)$, distinct from the VBS pattern at weak coupling. Differently from sVBS in the weak coupling regime arising from Fermi surface instability, the cVBS order is a consequence of strong electronic interaction. The results of the correlation-length ratio unambiguously establish the existence of the sVBS and cVBS long-range orders in the regions $J < 1.5$ and $J > 3.5$, respectively. Hence, for the intermediate fermion-component number $N = 4$, our simulation unequivocally reveals two different VBS ordered phases emerging in the weak and strong coupling regimes, with distinct patterns and underlying mechanisms.

The competition between various ordered phases with incompatible broken symmetries offers a promising route toward yielding an exotic QSL phase. In Eq. (1) for $N = 4$, the results of the correlation-length ratio reveal an intermediate phase in the region $1.5 < J < 3.5$, in which both the sVBS and cVBS orders are short range. The finite-size scaling of VBS structure factors with momentum (π, π) and $(\pi, 0)/(0, \pi)$, as depicted in Figs. 3(c) and 3(d), confirm the absence of VBS long-range ordering. We exclude the possibility of other SSB orderings occurring in this intermediate phase, including AFM, nematic, and hopping square orderings, by means of finite-scaling analysis of the structure factor as shown in Secs. IV, V, and VI of the Supplemental Material [103]. Furthermore, the correlation functions of VBS order exhibit exponentially decaying behavior, excluding the existence of a quasi-long-range order of VBS. The occurrence of intermediate phase in the absence of VBS long-range order is also witnessed by the momentum distribution of VBS structure factors, as shown in Fig. 4. In the weak-coupling ($J = 0.5$) and strong-coupling ($J = 5$) regimes, as expected, the VBS structure factors are sharply peaked at momenta (π, π) and $(\pi, 0)$, respectively. In the intermediate phase ($J = 2, 3$), the peaks of VBS structure factors are obviously broadened, implying the suppression of long-range ordering. In the intermediate disordered phase, the fluctuating short-range VBS orders with momenta $(\pi, 0)$ and $(0, \pi)$ are both present. The two states are easily tunneled to each other. The simultaneous presence of short-range x-bond VBS with momentum $(\pi, 0)$ and y-bond VBS with momentum $(0, \pi)$ gives rise to the short-range plaquette ordering with momenta in the diagonal direction. We present the results of correlation length for VBS order normalized by L, estimated from the relation $\xi = (1/\delta q)\sqrt{[S(Q)/S(Q + \delta q)] - 1}$, shown in Sec. IV of the Supplemental Material [103]. In the

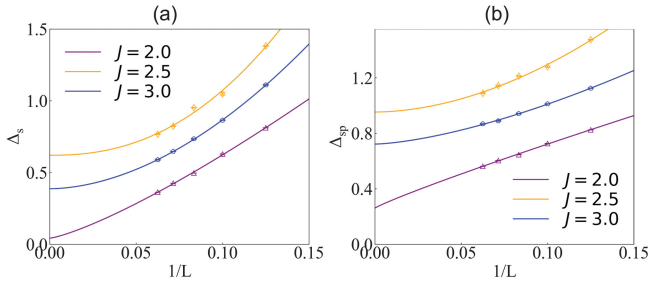

FIG. 5. Finite-size scaling of (a) the spin gap and (b) the single-particle gap in the intermediate symmetric phase for $N = 4$.

intermediate regime $1.5 < J < 3.5$, the correlation length is much smaller compared with the linear system size L, confirming that VBS order is short range and that our computational system is sufficiently large to capture the physical properties at the thermodynamic limit. Taken together, our simulation provides compelling evidences supporting the emergence of an intermediate phase without SSB for $N = 4$ in model Eq. (1).

To further investigate the nature of intermediate symmetric phase, we calculate the single-particle and spin gaps. The finite-size scaling results of spin and single-particle gaps for various values of J are shown in Figs. 5(a) and 5(b), respectively. The extrapolated values unambiguously reveal finite single-particle and spin gaps, demonstrating the nature of a Mott insulating phase, and possibly a gapped QSL featuring topological order. We also calculate the valence bond correlation function, excluding the possibility of algebraically decaying VBS order (see Sec. VII of the Supplemental Material [103]). Moreover, the gapped QSL is consistent with the Lieb-Schultz-Mattis theorem [112–115]. In our simulation, the average filling number is two electrons per unit cell; hence, the possibility of gapped SU(4) symmetric phase without ground-state degeneracy is excluded, owing to the LSM theorem for the SU(N) symmetric system [115]. In conclusion, our systematic simulations establish a possible gapped QSL phase existing in the intermediate interacting regime for $N = 4$. To further corroborate our conclusion and investigate how the QSL region evolves with N, we perform QMC simulations at $N = 5$ (see Sec. VIII of the Supplemental Material [103]). The results confirm that the conclusion for $SU(4)$ qualitatively holds at $N = 5$. More remarkably, the parameter regime of QSL is even larger with the increase of N to 5. The larger regime for $N = 5$ is possibly because the Dirac gapless QSL coupled to the $U(1)$ gauge field is a parent state of the gapped QSL unveiled in our study [116,117]. With increasing N, the scaling dimension of the monopole increases and the deconfined spinons are more stable, thus enlarging the parameter regime of QSL. The more rigorous studies are required to confirm the scenario, which is left for future work.

Discussions and concluding remarks.—In this Letter, we perform approximation-free numerical simulation to decipher the ground-state properties of a SU(N) fermionic model with SSH interaction on a square lattice. Various competing orderings emerge at varying interaction strength and the number of the fermion component N. At small values of N—namely, $N = 2$, 3—the ground state is an AFM ordered state. However, in the large-N limit, the dominant order is a VBS carrying momentum (π, π) while preserving spin rotational symmetry. The results at intermediate values of N are particularly intriguing. At $N = 4$, 5 with at weak coupling, the dominant VBS ordering is sVBS with momentum (π, π), persisting up to $J = 1.4(1.5)$, whereas the strong electronic interactions establish the VBS order carrying momentum $(\pi, 0)/(0, \pi)$ in the region $J > 3.5(5.4)$. More remarkably, in a large intermediate regime, an exotic Mott insulating phase without SSB develops. The intermediate symmetric Mott insulating phase possesses finite single-particle and spin gaps. All these features are consistent with a gapped QSL phase.

Notably, although we focus on the simulation on model in Eq. (1) at half filling, the model is sign-problem free at generic filling for even N. The possible superconductivity arising from doping various spontaneous symmetry-breaking phases or QSL is of particular interest. Furthermore, Eq. (1) is sign free at half filling for even N in the presence of repulsive Hubbard interaction, making it feasible to investigate the effect of Hubbard interactions on the various VBS and QSL orders unveiled in our simulation. For gapped QSL, topological entanglement entropy is the fingerprint to identify topological order, which exhibits a universal value $\gamma = -\ln N$ for the phase with Z_N topological order [118–120]. It is interesting to investigate entanglement properties through QMC simulation to determine the type of topological order in the intermediate QSL phase [121–126]. Another interesting direction to explore in the future is the nature of quantum phase transition between QSL and different VBS ordered phases. Therefore, our simulation paves a novel direction of constructing a concrete theoretically tractable model to investigate these crucial ingredients in quantum many-body physics.

We thank Hong Yao, Yi Zhou, Shou-Shu Gong, and Linhao Li for very helpful discussions. We thank the computational resources provided by the TianHe-1A supercomputer, the High Performance Computing Platform of Peking University, China. The QMC simulations are partly carried out with the ALF Library [127]. X.-J. Y. and L. X. are supported by the National Natural Science Foundation of China under Grant No. 11935002 and the National 973 project under Grant No. 2021YF1400501. Z. X. L. acknowledges support from the startup grant of Institute of Physics, Chinese Academy of Sciences.

*zixiangli@iphy.ac.cn

[1] S. Sachdev, *Quantum Phase Transitions*, 2nd ed. (Cambridge University Press, Cambridge, England, 2011), 10.1017/CBO9780511973765.
[2] E. Fradkin, *Field Theories of Condensed Matter Physics* (Cambridge University Press, Cambridge, England, 2013).
[3] P. A. Lee, N. Nagaosa, and X.-G. Wen, Rev. Mod. Phys. **78**, 17 (2006).
[4] E. Fradkin, S. A. Kivelson, and J. M. Tranquada, Rev. Mod. Phys. **87**, 457 (2015).
[5] S. Sachdev, Rev. Mod. Phys. **75**, 913 (2003).
[6] L. Balents, Nature (London) **464**, 199 (2010).
[7] P. A. Lee, Rep. Prog. Phys. **71**, 012501 (2007).
[8] Y. Zhou, K. Kanoda, and T.-K. Ng, Rev. Mod. Phys. **89**, 025003 (2017).
[9] L. Savary and L. Balents, Rep. Prog. Phys. **80**, 016502 (2016).
[10] M. R. Norman, Rev. Mod. Phys. **88**, 041002 (2016).
[11] C. Broholm, R. J. Cava, S. A. Kivelson, D. G. Nocera, M. R. Norman, and T. Senthil, Science **367**, eaay0668 (2020).
[12] M. Hermele, T. Senthil, M. P. A. Fisher, P. A. Lee, N. Nagaosa, and X.-G. Wen, Phys. Rev. B **70**, 214437 (2004).
[13] M. Hermele, T. Senthil, and M. P. A. Fisher, Phys. Rev. B **72**, 104404 (2005).
[14] S. Yan, D. A. Huse, and S. R. White, Science **332**, 1173 (2011).
[15] H.-C. Jiang, H. Yao, and L. Balents, Phys. Rev. B **86**, 024424 (2012).
[16] T.-H. Han, J. S. Helton, S. Chu, D. G. Nocera, J. A. Rodriguez-Rivera, C. Broholm, and Y. S. Lee, Nature (London) **492**, 406 (2012).
[17] F. L. Pratt, P. J. Baker, S. J. Blundell, T. Lancaster, S. Ohira-Kawamura, C. Baines, Y. Shimizu, K. Kanoda, I. Watanabe, and G. Saito, Nature (London) **471**, 612 (2011).
[18] Z. Meng, T. Lang, S. Wessel, F. Assaad, and A. Muramatsu, Nature (London) **464**, 847 (2010).
[19] S. Sorella, Y. Otsuka, and S. Yunoki, Sci. Rep. **2**, 992 (2012).
[20] H. J. Liao, Z. Y. Xie, J. Chen, Z. Y. Liu, H. D. Xie, R. Z. Huang, B. Normand, and T. Xiang, Phys. Rev. Lett. **118**, 137202 (2017).
[21] H. Yao and S. A. Kivelson, Phys. Rev. Lett. **99**, 247203 (2007).
[22] H. Yao and D.-H. Lee, Phys. Rev. Lett. **107**, 087205 (2011).
[23] Y.-F. Jiang, T. P. Devereaux, and H.-C. Jiang, Phys. Rev. B **100**, 165123 (2019).
[24] S.-S. Gong, W. Zhu, L. Balents, and D. N. Sheng, Phys. Rev. B **91**, 075112 (2015).
[25] Y. Zhou, P. A. Lee, T.-K. Ng, and F.-C. Zhang, Phys. Rev. Lett. **101**, 197201 (2008).
[26] Y.-C. He, M. P. Zaletel, M. Oshikawa, and F. Pollmann, Phys. Rev. X **7**, 031020 (2017).
[27] H.-K. Jin, R.-Y. Sun, H.-H. Tu, and Y. Zhou, Sci. Bull. **67**, 918 (2022).
[28] Y.-C. Wang, Z. Yan, C. Wang, Y. Qi, and Z. Y. Meng, Phys. Rev. B **103**, 014408 (2021).
[29] Z. Yan, Y.-C. Wang, N. Ma, Y. Qi, and Z. Y. Meng, npj Quantum Mater. **6**, 1 (2021).
[30] Y. Wan and O. Tchernyshyov, Phys. Rev. B **87**, 104408 (2013).
[31] X.-Y. Song, C. Wang, A. Vishwanath, and Y.-C. He, Nat. Commun. **10**, 4254 (2019).
[32] Y.-C. Wang, X.-F. Zhang, F. Pollmann, M. Cheng, and Z. Y. Meng, Phys. Rev. Lett. **121**, 057202 (2018).
[33] A. Szasz, J. Motruk, M. P. Zaletel, and J. E. Moore, Phys. Rev. X **10**, 021042 (2020).
[34] B.-B. Chen, Z. Chen, S.-S. Gong, D. N. Sheng, W. Li, and A. Weichselbaum, Phys. Rev. B **106**, 094420 (2022).
[35] N. Read and S. Sachdev, Nucl. Phys. **316B**, 609 (1989).
[36] N. Read and S. Sachdev, Phys. Rev. Lett. **62**, 1694 (1989).
[37] T. C. Lang, Z. Y. Meng, A. Muramatsu, S. Wessel, and F. F. Assaad, Phys. Rev. Lett. **111**, 066401 (2013).
[38] F. F. Assaad, Phys. Rev. B **71**, 075103 (2005).
[39] R. K. Kaul and A. W. Sandvik, Phys. Rev. Lett. **108**, 137201 (2012).
[40] Z. Zhou, D. Wang, Z. Y. Meng, Y. Wang, and C. Wu, Phys. Rev. B **93**, 245157 (2016).
[41] P. Patil, F. Alet, S. Capponi, and M. Mambrini, Phys. Rev. B **105**, L140403 (2022).
[42] P. Corboz, M. Lajkó, A. M. Läuchli, K. Penc, and F. Mila, Phys. Rev. X **2**, 041013 (2012).
[43] A. Koga, S. Nakauchi, and J. Nasu, Phys. Rev. B **97**, 094427 (2018).
[44] C. Honerkamp and W. Hofstetter, Phys. Rev. Lett. **92**, 170403 (2004).
[45] G. Chen and C. Wu, arXiv:2112.02630.
[46] H. Xu, Y. Wang, Z. Zhou, and C. Wu, arXiv:1912.11791.
[47] Z. Cai and C. Wu, arXiv:2003.08566.
[48] D. Wang, L. Wang, and C. Wu, Phys. Rev. B **100**, 115155 (2019).
[49] Z. Zhou, C. Wu, and Y. Wang, Phys. Rev. B **97**, 195122 (2018).
[50] S. Xu, J. T. Barreiro, Y. Wang, and C. Wu, Phys. Rev. Lett. **121**, 167205 (2018).
[51] R. K. Kaul, R. G. Melko, and A. W. Sandvik, Annu. Rev. Condens. Matter Phys. **4**, 179 (2013).
[52] P. Nataf, M. Lajkó, A. Wietek, K. Penc, F. Mila, and A. M. Läuchli, Phys. Rev. Lett. **117**, 167202 (2016).
[53] Z. Zhou, Z. Cai, C. Wu, and Y. Wang, Phys. Rev. B **90**, 235139 (2014).
[54] D. Wang, Y. Li, Z. Cai, Z. Zhou, Y. Wang, and C. Wu, Phys. Rev. Lett. **112**, 156403 (2014).
[55] Z. Cai, H.-H. Hung, L. Wang, and C. Wu, Phys. Rev. B **88**, 125108 (2013).
[56] Z. Cai, H.-h. Hung, L. Wang, D. Zheng, and C. Wu, Phys. Rev. Lett. **110**, 220401 (2013).
[57] P. Nataf and F. Mila, Phys. Rev. Lett. **113**, 127204 (2014).
[58] H.-H. Hung, Y. Wang, and C. Wu, Phys. Rev. B **84**, 054406 (2011).
[59] M. Raczkowski and F. F. Assaad, Phys. Rev. Res. **2**, 013276 (2020).
[60] F. H. Kim, F. F. Assaad, K. Penc, and F. Mila, Phys. Rev. B **100**, 085103 (2019).

[61] Y. Da Liao, X. Y. Xu, Z. Y. Meng, and Y. Qi, Phys. Rev. B **106**, 075111 (2022).
[62] Y. Da Liao, X. Y. Xu, Z. Y. Meng, and Y. Qi, Phys. Rev. B **106**, 115149 (2022).
[63] X. Zhu, Y. Huang, H. Guo, and S. Feng, Phys. Rev. B **106**, 075109 (2022).
[64] K. S. D. Beach, F. Alet, M. Mambrini, and S. Capponi, Phys. Rev. B **80**, 184401 (2009).
[65] K. Harada, N. Kawashima, and M. Troyer, Phys. Rev. Lett. **90**, 117203 (2003).
[66] X.-P. Yao, R. L. Luo, and G. Chen, Phys. Rev. B **105**, 024401 (2022).
[67] F. F. Assaad and T. Grover, Phys. Rev. X **6**, 041049 (2016).
[68] L. Janssen and U. F. P. Seifert, Phys. Rev. B **105**, 045120 (2022).
[69] K. Yamamoto and N. Kawakami, Phys. Rev. B **107**, 045110 (2023).
[70] S.-Y. Wang, D. Wang, and Q.-H. Wang, Phys. Rev. B **106**, 245113 (2022).
[71] E. Ibarra-García-Padilla, S. Dasgupta, H.-T. Wei, S. Taie, Y. Takahashi, R. T. Scalettar, and K. R. A. Hazzard, Phys. Rev. A **104**, 043316 (2021).
[72] H. Yoshida and H. Katsura, Phys. Rev. Lett. **126**, 100201 (2021).
[73] C. Romen and A. M. Läuchli, Phys. Rev. Res. **2**, 043009 (2020).
[74] P. Fromholz and P. Lecheminant, Phys. Rev. B **102**, 094410 (2020).
[75] B. J. DeSalvo, M. Yan, P. G. Mickelson, Y. N. Martinez de Escobar, and T. C. Killian, Phys. Rev. Lett. **105**, 030402 (2010).
[76] A. V. Gorshkov, M. Hermele, V. Gurarie, C. Xu, P. S. Julienne, J. Ye, P. Zoller, E. Demler, M. D. Lukin, and A. M. Rey, Nat. Phys. **6**, 289 (2010).
[77] S. Taie, Y. Takasu, S. Sugawa, R. Yamazaki, T. Tsujimoto, R. Murakami, and Y. Takahashi, Phys. Rev. Lett. **105**, 190401 (2010).
[78] J. S. Krauser, J. Heinze, N. Fläschner, S. Götze, O. Jürgensen, D.-S. Lühmann, C. Becker, and K. Sengstock, Nat. Phys. **8**, 813 (2012).
[79] S. Taie, R. Yamazaki, S. Sugawa, and Y. Takahashi, Nat. Phys. **8**, 825 (2012).
[80] G. Pagano, M. Mancini, G. Cappellini, P. Lombardi, F. Schäfer, H. Hu, X.-J. Liu, J. Catani, C. Sias, M. Inguscio, and L. Fallani, Nat. Phys. **10**, 198 (2014).
[81] C. Hofrichter, L. Riegger, F. Scazza, M. Höfer, D. R. Fernandes, I. Bloch, and S. Fölling, Phys. Rev. X **6**, 021030 (2016).
[82] Y. Cao, V. Fatemi, A. Demir, S. Fang, S. L. Tomarken, J. Y. Luo, J. D. Sanchez-Yamagishi, K. Watanabe, T. Taniguchi, E. Kaxiras, R. C. Ashoori, and P. Jarillo-Herrero, Nature (London) **556**, 80 (2018).
[83] Y. Cao, V. Fatemi, S. Fang, K. Watanabe, T. Taniguchi, E. Kaxiras, and P. Jarillo-Herrero, Nature (London) **556**, 43 (2018).
[84] R. Bistritzer and A. H. MacDonald, Proc. Natl. Acad. Sci. U.S.A. **108**, 12233 (2011).
[85] D. V. Chichinadze, L. Classen, Y. Wang, and A. V. Chubukov, Phys. Rev. Lett. **128**, 227601 (2022).
[86] X. Y. Xu, K. T. Law, and P. A. Lee, Phys. Rev. B **98**, 121406(R) (2018).
[87] Y. Da Liao, Z. Y. Meng, and X. Y. Xu, Phys. Rev. Lett. **123**, 157601 (2019).
[88] Y.-Z. You and A. Vishwanath, npj Quantum Mater. **4**, 16 (2019).
[89] Z.-X. Li, Y.-F. Jiang, and H. Yao, Phys. Rev. B **91**, 241117(R) (2015).
[90] Z.-X. Li, Y.-F. Jiang, and H. Yao, Phys. Rev. Lett. **117**, 267002 (2016).
[91] L. Wang, Y.-H. Liu, M. Iazzi, M. Troyer, and G. Harcos, Phys. Rev. Lett. **115**, 250601 (2015).
[92] Z. C. Wei, C. Wu, Y. Li, S. Zhang, and T. Xiang, Phys. Rev. Lett. **116**, 250601 (2016).
[93] F. Assaad and H. Evertz, in *Computational Many-Particle Physics* (Springer, New York, 2008), pp. 277–356.
[94] R. Blankenbecler, D. J. Scalapino, and R. L. Sugar, Phys. Rev. D **24**, 2278 (1981).
[95] Z.-X. Li and H. Yao, Annu. Rev. Condens. Matter Phys. **10**, 337 (2019).
[96] N. Read and S. Sachdev, Phys. Rev. Lett. **66**, 1773 (1991).
[97] X. G. Wen, Phys. Rev. B **44**, 2664 (1991).
[98] X. Chen, Z.-C. Gu, and X.-G. Wen, Phys. Rev. B **82**, 155138 (2010).
[99] X.-G. Wen, Int. J. Mod. Phys. B **04**, 239 (1990).
[100] Z.-X. Li, Y.-F. Jiang, S.-K. Jian, and H. Yao, Nat. Commun. **8**, 1 (2017).
[101] W. P. Su, J. R. Schrieffer, and A. J. Heeger, Phys. Rev. Lett. **42**, 1698 (1979).
[102] E. Fradkin and J. E. Hirsch, Phys. Rev. B **27**, 1680 (1983).
[103] See Supplemental Material at http://link.aps.org/supplemental/10.1103/PhysRevLett.132.036704 for the details of numerical calculations.
[104] L. Wang, P. Corboz, and M. Troyer, New J. Phys. **16**, 103008 (2014).
[105] Z.-X. Li, Y.-F. Jiang, and H. Yao, New J. Phys. **17**, 085003 (2015).
[106] B.-H. Li, Z.-X. Li, and H. Yao, Phys. Rev. B **101**, 085105 (2020).
[107] Y.-X. Zhang, H.-M. Guo, and R. T. Scalettar, Phys. Rev. B **101**, 205139 (2020).
[108] X. Cai, Z.-X. Li, and H. Yao, Phys. Rev. Lett. **127**, 247203 (2021).
[109] X. Cai, Z.-X. Li, and H. Yao, Phys. Rev. B **106**, L081115 (2022).
[110] A. Götz, S. Beyl, M. Hohenadler, and F. F. Assaad, Phys. Rev. B **105**, 085151 (2022).
[111] C. Feng, B. Xing, D. Poletti, R. Scalettar, and G. Batrouni, Phys. Rev. B **106**, L081114 (2022).
[112] E. Lieb, T. Schultz, and D. Mattis, Ann. Phys. (N.Y.) **16**, 407 (1961).
[113] M. Oshikawa, Phys. Rev. Lett. **84**, 3370 (2000).
[114] M. B. Hastings, Phys. Rev. B **69**, 104431 (2004).
[115] Y. Yao and M. Oshikawa, Phys. Rev. X **10**, 031008 (2020).
[116] X.-Y. Song, Y.-C. He, A. Vishwanath, and C. Wang, Phys. Rev. X **10**, 011033 (2020).
[117] X.-Y. Song, C. Wang, A. Vishwanath, and Y.-C. He, Nat. Commun. **10**, 4254 (2019).

[118] A. Kitaev and J. Preskill, Phys. Rev. Lett. **96**, 110404 (2006).
[119] M. Levin and X.-G. Wen, Phys. Rev. Lett. **96**, 110405 (2006).
[120] H. Watanabe, M. Cheng, and Y. Fuji, J. Math. Phys. (N.Y.) **64** (2023).
[121] M. B. Hastings, I. González, A. B. Kallin, and R. G. Melko, Phys. Rev. Lett. **104**, 157201 (2010).
[122] T. Grover, Phys. Rev. Lett. **111**, 130402 (2013).
[123] F. F. Assaad, Phys. Rev. B **91**, 125146 (2015).
[124] J. Zhao, B.-B. Chen, Y.-C. Wang, Z. Yan, M. Cheng, and Z. Y. Meng, npj Quantum Mater. **7**, 69 (2022).
[125] J. D'Emidio, R. Orus, N. Laflorencie, and F. de Juan, arXiv:2211.04334.
[126] G. Pan, Y. Da Liao, W. Jiang, J. D'Emidio, Y. Qi, and Z. Y. Meng, Phys. Rev. B **108**, L081123 (2023).
[127] F. F. Assaad, M. Bercx, F. Goth, A. Götz, J. S. Hofmann, E. Huffman, Z. Liu, F. P. Toldin, J. S. E. Portela, and J. Schwab, SciPost Phys. Codebases **1** (2022).